WATER RESOURCES RESEARCH, VOL. 19, NO. 3, PAGES 691-700, JUNE 1983

Modeling Tritium and Chloride 36 Transport Through an Aggregated Oxisol

P. NKEDI-KIZZA,[1,2] J. W. BIGGAR,[1] M. TH. VAN GENUCHTEN,[3] P. J. WIERENGA,[4] H. M. SELIM,[5] J. M. DAVIDSON,[6] AND D. R. NIELSEN[1]

Breakthrough curves (BTC's) of ^3H_2O and ^{36}Cl simultaneously displaced through columns of various-sized aggregates of an Ione Oxisol soil were measured under water-saturated steady flow conditions. The data were simulated using two conceptual models. In model I, all soil water was assumed to be mobile with a physical equilibrium existing in the system. For model II, soil water was partitioned into mobile and immobile regions. Convective diffusive solute transport was limited to the mobile water region. Transfer of a tracer between the two soil water regions was assumed to occur at a rate proportional to the difference in tracer concentration between the two regions. Sorption of ^3H_2O and ^{36}Cl was considered to be an instantaneous linear and reversible process. The two unknown parameters in model I and the four unknown parameters in model II were estimated by fitting model predictions to the experimental data. Model I could only describe BTC's obtained from columns packed with small aggregates (0.5–1 mm) and for displacements run at small fluxes (0.2 cm/h), whereas model II described all the BTC's well. Peclet numbers P in model II, as measured on each separate column, were essentially constant, indicating a linear relationship between the apparent diffusion coefficient D and the mobile pore water velocity v_m. The fraction of soil water that is mobile, ϕ, and the mass transfer coefficient α were found to be a function of the physical and chemical properties of the porous medium (aggregate size, pore water velocity, and solution concentration).

INTRODUCTION

Asymmetry and tailing of breakthrough curves (BTC's) for solutes leached through aggregated porous media under water saturated conditions have been reported by *Biggar and Nielsen* [1962], *DeSmedt* [1979], *Rao et al.* [1980*a*], and *Nkedi-Kizza et al.* [1982]. Several transport models have been proposed to account for the observed asymmetry especially in the case of nonadsorbed solutes. A common characteristic of most of these models is the assumption that there are two distinct soil water regions in the system: one region designated as the 'mobile' water region, where solute transport takes place by convection and diffusion, and another region, designated as the 'immobile' region, where solute transfer takes place by diffusion only. Differences between the various models arise because of different assumptions regarding the exact form and location of this stagnant water in the system.

In one approach, stagnant water has been equated with water films surrounding the particles; solutes are being transferred into and out of the films by diffusion according to Fick's law [*Boyd et al.*, 1947; *Gottschlich*, 1963; *Skopp and Warrick*, 1974]. The film thickness in this approach can be estimated from BTC data. Another approach considers the stagnant water regions to include films surrounding the aggregates and the intra-aggregate pore water regions. Thus solute transfer into and out of the stagnant water regions occurs by both film and aggregate diffusion [*Boyd et al.*, 1947; *Hiester and Vermeulen*, 1952; *Lapidus and Amundson*, 1952; *Gilliland and Baddour*, 1953]. In this approach the aggregate size and shape is known but the film thickness must be estimated from BTC data.

A third approach assumes that all water between the aggregates is mobile and that stagnant water is located exclusively within the aggregates (intra-aggregate pore water) [*Rao et al.*, 1980*a*; *Nkedi-Kizza et al.*, 1982]. Here, the transfer of solutes in and out of the stagnant water regions is described by Fick's second law of diffusion. *Nkedi-Kizza et al.* [1982] assigned a distinct geometry to the stagnant water regime and estimated the mobile water content independently by draining the column at a pressure head of −80 cm of water.

Owing to uncertainty about understanding the actual shapes and sizes of aggregates, whether packed in a column or in the field, a more practical approach has been to assume that solute transfer between the mobile and stagnant water regions can be modeled as a simple first-order exchange process [*Coats and Smith*, 1964; *Raats*, 1973; *van Genuchten and Wierenga*, 1976; *Gaudet et al.*, 1977; *DeSmedt and Wierenga*, 1979*a*, *b*]. Convective-diffusive solute transport is again limited to the mobile water regions, whereas diffusive mass transfer between the mobile and stagnant water regions is assumed to be proportional to the concentration difference between the two soil water phases.

The presence of immobile or stagnant water in the system can be attributed to the physical configuration of the aggregates; the nonequilibrium situation, if present, is therefore an apparent physical phenomenon [*van Genuchten*, 1981]. In order to verify the assumption of physical nonequilibrium and to investigate the tendencies of model parameters with variation in experimental conditions, a series of miscible displacement experiments were carried out using an aggregated Oxisol as the porous medium and ^{36}Cl and ^3H_2O as the solute tracers. The experiments were carried out with different aggregate sizes and run at different flow rates. The particular tracer-soil combinations used in this study resulted in a weakly adsorptive system. Because of adsorption,

[1] Department of Land, Air, and Water Resources, University of California, Davis, California 95616.
[2] Now at the Department of Soil Science, University of Florida, Gainesville, Florida 32611.
[3] U.S. Salinity Laboratory, U.S. Department of Agriculture, Riverside, California 92501.
[4] Department of Agronomy, New Mexico State University, Las Cruces, New Mexico 88003.
[5] Department of Agronomy, Louisiana State University, Baton Rouge, Louisiana 70803.
[6] Department of Soil Science, University of Florida, Gainesville, Florida 32611.

Paper number 3W0349.
0043-1397/83/003W-0349$05.00

the formulation of *van Genuchten and Wierenga* [1976] is used here. The model, expressed in dimensionless variables is given by

$$\beta R \frac{\partial C_1}{\partial T} + (1 - \beta)R \frac{\partial C_2}{\partial T} = \frac{1}{P} \frac{\partial^2 C_1}{\partial x^2} - \frac{\partial C_1}{\partial x} \tag{1}$$

$$(1 - \beta)R \frac{\partial C_2}{\partial T} = \omega(C_1 - C_2) \tag{2}$$

where

$$T = \frac{vt}{L} = \frac{v_m t \phi}{L} \tag{3}$$

$$x = \frac{z}{L} \tag{4}$$

$$\phi = \frac{\theta_m}{\theta} \qquad \theta = \theta_m + \theta_{im} \tag{5}$$

$$C_1 = \frac{C_m}{C_0} \qquad C_2 = \frac{C_{im}}{C_0} \tag{6}$$

$$\mathrm{P} = \frac{v_m L}{D} \qquad v_m = \frac{q}{\theta_m} \tag{7}$$

$$\omega = \frac{\alpha L}{v_m \theta_m} = \frac{\alpha L}{q} \tag{8}$$

$$R_m = 1 + \frac{\rho f K_D}{\theta_m} \qquad R = 1 + \frac{\rho K_D}{\theta} \tag{9}$$

$$\beta = \frac{\theta_m + \rho f K_D}{\theta + \rho K_D} = \frac{\theta_m R_m}{R\theta} = \frac{\phi R_m}{R} \tag{10}$$

The terms and symbols used in (1)–(13) are defined in the notation section at the end of the paper. The assumed initial and boundary conditions for this study are

$$\lim_{x \to 0} \left[C_1 - \frac{1}{P} \frac{\partial C_1}{\partial x} \right] = 1 \qquad 1 < T \leq T_1$$

$$\lim_{x \to 0} \left[C_1 - \frac{1}{P} \frac{\partial C_1}{\partial x} \right] = 0 \qquad T > T_1 \tag{11}$$

$$\lim_{x \to \infty} [C_1(x, T)] = 0 \tag{12}$$

$$C_1(x, 0) = C_2(x, 0) = 0 \tag{13}$$

The analytical solution to (1)–(13) has been given by *van Genuchten and Wierenga* [1976].

If we assume that all soil water participates in the convective-diffusive process ($\phi = 1$) and, in addition, assume that all adsorption sites are equally accessible to the displacing fluid ($f = 1$), then (1) and (2) simplify to [*Lindstrom et al.*, 1967]

$$R \frac{\partial C_1}{\partial T} = \frac{1}{P} \frac{\partial^2 C_1}{\partial x^2} - \frac{\partial C_1}{\partial x} \tag{14}$$

This more simple equation has been the more standard model for describing solute transport. We will refer to (14) as model I, whereas (1) and (2) will be referred to as model II. The applicability of both models to the experimental data will be discussed.

MATERIALS AND METHODS

Miscible Displacement Experiments

The Ione soil from the Eocene formation of California and recently classified as an Oxisol by *Singer and Nkedi-Kizza* [1980] was used in this study. The soil is strongly aggregated, has a *p*H of 3.7, a CEC of 2 meq/100 g soil, a Fe_2O_3 content of 6.5%, a zero point of charge (ZPC) at *p*H 3.6, and has kaolinite as the predominant clay mineral. More detailed descriptions of the physical and chemical properties of the soil are given by Singer and Nkedi-Kizza.

The procedure followed to adjust the soil to a *p*H of 7 and the separation of the calcium saturated soil into aggregate fractions of 0.5–1.0, 1–2 and 2–4.7 mm has been described by *Nkedi-Kizza* [1979]. Each aggregate fraction was packed into acrylic plastic cylinders, 5 cm long and 7.6 cm in diameter. Miscible displacement techniques, similar to those described by Nkedi-Kizza were employed to measure effluent BTC's for three tracers (^{36}Cl, ^3H_2O, and ^{45}Ca) applied simultaneously in one pulse. The BTC's were obtained using 0.001, 0.01, or 0.1 *N* $CaCl_2$ solutions adjusted to a *p*H of 7. The electrolyte solutions were spiked with three radioactive tracers, each giving about 5 nCi/ml. Since each effluent aliquot contained three tracers, the technique of triple labeling was followed during the liquid scintillation determination of each tracer (P. Nkedi-Kizza et al., unpublished manuscript, 1983). The relevant data for the various ^3H_2O and ^{36}Cl displacement experiments are listed in Table 1. The ^{45}Ca BTC data are not included in this paper. The small velocity displacements were carried out first at a concentration of 0.1 N $CaCl_2$ and then followed by 0.01 N and 0.001 N, respectively; the larger flow velocity experiments were run subsequently in a similar order of solution concentrations. All columns had similar bulk densities ρ and saturated water contents θ. The input pulse T_1 of tracer varied from one displacement experiment to another.

Model Parameter Estimation

Model II (equations (1) and (2)) contains four independent parameters (P, R, β, and ω). Experimental methods are currently unavailable to measure parameters β and ω independently in this model. Although it is possible to estimate R independently (e.g., by means of batch equilibrium techniques), least square methods were used to estimate P and R in addition to β and ω.

The four model parameters were estimated using the nonlinear least squares curve-fitting program of *van Genuchten* [1981]. The curve-fitting program is written such that up to five parameters (P, R, β, ω, and T_1) can be optimized simultaneously. However, the pulse pore volume T_1 was accurately measured during the experiments and did not require adjustment. Fitted values of the remaining parameters are given in Table 2. The same program of van Genuchten was also used to estimate the parameters P and R in model I (Table 3).

Estimates for the original variables can be obtained once the dimensionless parameters are fitted to the data. For example, the distribution coefficient K_D can be calculated from the fitted value of R by using (9). Similarly, the value of

TABLE 1. Soil Column Data for Various Displacements Through the Ione Oxisol at pH 7

Experiment Number	Aggregate Diameter, mm	Solution Concentration, N	Bulk Density ρ, g cm^{-3}	Water Content θ, cm^3 cm^{-3}	Flux q, cm h^{-1}	Pulse T_1 Pore Volume
			Column 1			
1	0.5–1	0.1	1.238	0.579	0.254	0.376
2	0.5–1	0.01	1.238	0.579	0.254	0.510
3	0.5–1	0.001	1.238	0.579	0.256	0.555
4	0.5–1	0.1	1.238	0.579	3.413	0.501
5	0.5–1	0.01	1.238	0.579	3.107	0.422
6	0.5–1	0.001	1.238	0.579	0.079	0.461
			Column 2			
7	1–2	0.1	1.249	0.576	0.254	0.349
8	1–2	0.01	1.249	0.576	0.254	0.502
9	1–2	0.001	1.249	0.576	0.256	0.474
10	1–2	0.01	1.249	0.576	3.418	0.357
11	1–2	0.001	1.249	0.576	3.405	0.470
			Column 3			
12	2–4.7	0.1	1.238	0.576	0.256	0.352
13	2–4.7	0.01	1.238	0.576	0.251	0.391
14	2–4.7	0.001	1.238	0.576	0.256	0.388
15	2–4.7	0.1	1.238	0.576	3.203	0.391
16	2–4.7	0.01	1.238	0.576	2.819	0.422
17	2–4.7	0.001	1.238	0.576	3.283	0.413

D follows from P by making use of (7), whereas α follows from (8) from ω is known. Unfortunately, the parameters ϕ and f cannot be obtained from one displacement experiment alone. This is because both parameters are included in the dimensionless factor β and hence have similar effects on the position and shape of the BTC. From (9) and (10),

$$\phi = \beta R - f(R - 1) \tag{15}$$

To calculate ϕ from (15), an estimate for f is first needed. Although tritiated water and chloride may have the same ϕ values, the value of f is not necessarily the same because of different locations of their adsorption sites in the aggregated soil. Considering that the exterior surface area of soil aggregates is much less than the interior surface area, *Nkedi-Kizza et al.* [1982] and P. C. S. Rao and R. E. Jessup (unpublished manuscript, 1983) simply used a value of zero for f. This approach assumes that tracer adsorption takes place only inside the stagnant region of the soil (inside the aggregates). As an alternative, one could, as a first approximation, also assume that f and ϕ are numerically equal and hence that they are similar functions of the physical makeup of the porous medium. An advantage of this approach is that in the limit when all soil water becomes mobile ($\phi = 1$), all adsorption sites also become available for the displacing fluid ($f = 1$). In that case, model II reduces to model I. Assuming that $\phi = f$ leads to the simple rule $\phi = f = \beta$. In this study the retardation factor R is always close to 1 (Tables 2, 3). It follows, therefore, from (15) that an accurate value of f is not crucial when estimating ϕ from curve-fitted values of R and β. Here we assume that $f = \phi$. From (15) it follows, therefore, that

$$\phi = \beta \tag{16}$$

RESULTS AND DISCUSSION

An agreement between model simulation and experimental data is generally taken as a verification of the conceptual processes which form the basis of the model. Verification of conceptual processes in the model should be valid only when all model parameters are measured or estimated independently of the BTC data being simulated. When experimental techniques are inadequate to measure parameters independently, they are frequently estimated on the basis of a best fit of the model to the experimental data [*van Genuchten et al.*, 1977; *O'Connor et al.*, 1976; *Rao et al.*, 1979; *DeSmedt*, 1979]. This technique is useful in parameter estimation but does not ensure process identification [*Davidson et al.*, 1980; *Rao et al.*, 1980*b*]. In this study we were aware of such considerations but chose to simulate each BTC with the two models and then see if there is dependency of model parameters on the physical (flux and aggregate size) and chemical (concentration) conditions of the porous media.

The basic difference between model I and model II is that in model I, all water in the system is considered to be contributing to convective solute transport, whereas in model II, only the mobile water phase is assumed to be involved

TABLE 2. Curve-Fitted Dimensionless Parameter Values Using Model I

Experiment Number	P		R	
	^{36}Cl	^3H_2O	^{36}Cl	^3H_2O
1	3.3 ± 0.2	4.3 ± 0.2	1.078 ± 0.021	1.103 ± 0.015
2	3.4 ± 0.2	4.2 ± 0.2	1.129 ± 0.016	1.206 ± 0.015
3	3.0 ± 0.1	2.5 ± 0.3	0.963 ± 0.005	1.121 ± 0.061
4	6.4 ± 0.3	7.9 ± 0.2	1.286 ± 0.016	1.268 ± 0.011
5	2.7 ± 0.3	2.6 ± 0.2	0.794 ± 0.029	0.845 ± 0.024
6	3.8 ± 0.2	3.4 ± 0.2	0.830 ± 0.029	0.903 ± 0.030
7	3.7 ± 0.2	4.4 ± 0.3	0.991 ± 0.032	1.006 ± 0.020
8	7.8 ± 0.6	13.3 ± 0.6	1.525 ± 0.031	1.331 ± 0.012
9	5.0 ± 0.3	5.0 ± 0.6	0.798 ± 0.034	0.869 ± 0.032
10	7.9 ± 1.7	10.4 ± 1.7	0.650 ± 0.031	0.672 ± 0.022
11	5.0 ± 0.9	8.3 ± 1.1	0.614 ± 0.028	0.626 ± 0.015
12	2.2 ± 0.1	2.8 ± 0.1	0.880 ± 0.020	0.890 ± 0.011
13	1.9 ± 0.1	2.6 ± 0.1	0.877 ± 0.027	0.938 ± 0.016
14	4.1 ± 0.4	4.3 ± 0.7	0.953 ± 0.031	0.918 ± 0.041
15	6.0 ± 0.6	7.2 ± 0.6	0.853 ± 0.021	0.865 ± 0.015
16	3.1 ± 0.7	3.0 ± 0.7	0.779 ± 0.059	0.746 ± 0.054
17	2.8 ± 0.4	3.0 ± 0.5	0.950 ± 0.050	0.850 ± 0.040

TABLE 3. Curve-Fitted Dimensionless Parameter Values Using Model II

Experiment Number	P		R		β		ω	
	^{36}Cl	$^{3}H_2O$	^{36}Cl	$^{3}H_2O$	^{36}Cl	$^{3}H_2O$	^{36}Cl	$^{3}H_2O$
1	3.6 ± 0.2	4.6 ± 0.3	1.072 ± 0.022	1.096 ± 0.014	0.901 ± 0.003	0.917 ± 0.004	1.089 ± 0.046	0.917 ± 0.039
2	3.7 ± 0.1	4.7 ± 0.3	1.135 ± 0.017	1.204 ± 0.016	0.905 ± 0.001	0.893 ± 0.058	0.916 ± 0.060	0.885 ± 0.666
3	4.4 ± 0.8	3.1 ± 0.2	0.993 ± 0.025	1.123 ± 0.036	0.672 ± 0.145	0.900 ± 0.004	2.008 ± 1.010	0.773 ± 0.827
4	9.1 ± 2.7	9.5 ± 3.3	1.293 ± 0.026	1.269 ± 0.046	0.712 ± 0.229	0.835 ± 0.013	2.646 ± 2.470	1.781 ± 4.149
5	6.9 ± 0.1	5.1 ± 0.8	1.063 ± 0.041	1.077 ± 0.037	0.578 ± 0.018	0.650 ± 0.042	0.669 ± 0.064	0.510 ± 0.134
6	10.1 ± 1.1	8.1 ± 1.1	1.111 ± 0.028	1.186 ± 0.037	0.596 ± 0.020	0.608 ± 0.026	0.619 ± 0.072	0.611 ± 0.100
7	7.3 ± 1.0	6.8 ± 0.7	1.268 ± 0.049	1.187 ± 0.035	0.650 ± 0.033	0.749 ± 0.034	0.490 ± 0.115	0.362 ± 0.120
8	14.4 ± 1.4	13.2 ± 1.4	1.495 ± 0.041	1.319 ± 0.018	0.781 ± 0.003	0.955 ± 0.003	2.128 ± 1.059	0.955 ± 0.049
9	9.3 ± 1.7	7.7 ± 1.5	1.128 ± 0.128	1.144 ± 0.139	0.644 ± 0.060	0.706 ± 0.071	0.307 ± 0.115	0.249 ± 0.135
10	21.3 ± 4.1	18.9 ± 1.3	0.946 ± 0.061	0.912 ± 0.042	0.612 ± 0.034	0.688 ± 0.027	0.446 ± 0.087	0.308 ± 0.041
11	10.8 ± 0.7	10.2 ± 1.8	1.021 ± 0.086	0.813 ± 0.085	0.554 ± 0.043	0.718 ± 0.066	0.309 ± 0.033	0.211 ± 0.089
12	2.4 ± 0.4	4.0 ± 0.6	0.879 ± 0.023	0.916 ± 0.012	0.873 ± 0.137	0.717 ± 0.087	0.968 ± 1.252	1.670 ± 0.900
13	2.9 ± 0.2	3.1 ± 0.1	1.036 ± 0.064	0.990 ± 0.080	0.746 ± 0.067	0.870 ± 0.073	0.378 ± 0.230	0.247 ± 0.115
14	8.9 ± 2.8	14.4 ± 2.7	1.203 ± 0.135	1.233 ± 0.051	0.641 ± 0.125	0.544 ± 0.047	0.568 ± 0.416	0.850 ± 0.156
15	8.1 ± 2.0	9.4 ± 2.8	0.986 ± 0.086	0.907 ± 0.043	0.806 ± 0.079	0.882 ± 0.107	0.222 ± 0.23	0.298 ± 0.521
16	14.4 ± 1.4	14.6 ± 1.4	1.323 ± 0.053	1.254 ± 0.038	0.441 ± 0.016	0.447 ± 0.014	0.732 ± 0.054	0.741 ± 0.042
17	12.5 ± 1.9	10.8 ± 0.7	1.384 ± 0.035	1.262 ± 0.045	0.465 ± 0.019	0.500 ± 0.030	0.951 ± 0.086	0.751 ± 0.039

in convective transport. For both models the model parameters were obtained by the least squares optimization techniques. Model I contains two parameters, P and R, whereas model II contains four parameters, P, R, β, and ω.

In all figures the experimental BTC's are presented as dots and the calculated BTC's are shown as solid lines. The measured BTC's for $^{3}H_2O$ and ^{36}Cl displacement through a soil column packed with aggregates of 0.5–1.0 mm at a flux of 0.25 cm/h are shown in Figures 1 and 2, respectively. The data are from experiments 1–3 (Table 1). The difference between experiments 1, 2, and 3 is the concentration of the carrier solution, $CaCl_2$. Model I describes the experimental data well for both $^{3}H_2O$ and ^{36}Cl. The BTC's of both tracers with the simulations of model I for the soil column packed with aggregate fractions of 2–4.7 mm and the displacement run at a flux of about 3 cm/h are presented in Figures 3 and 4.

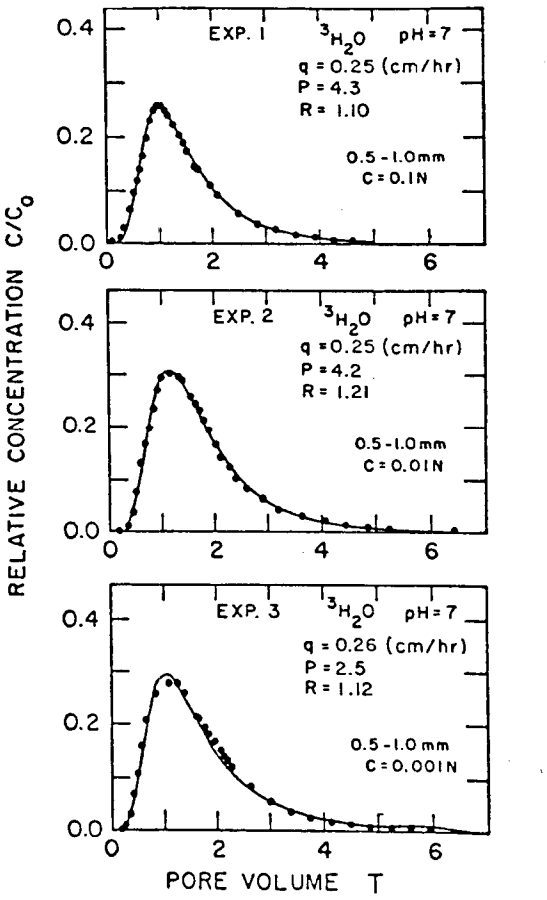

Fig. 1. Measured $^{3}H_2O$ breakthrough curves through column 1. The dots represent experimental data points, and the lines are calculated with model I.

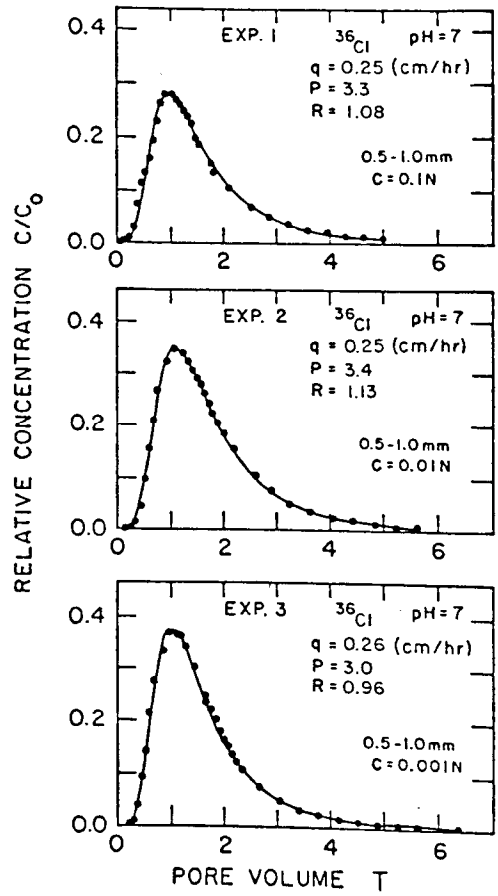

Fig. 2. Measured ^{36}Cl breakthrough curves through column 1. The dots represent experimental data points, and the lines are calculated with model I.

The data are from experiments 15–17 (Table 1). In this case the model fails to describe the BTC's, especially the tailing position of the BTC's. For both tracers the R values (Table 2) are much less than 1, which implies that negative adsorption is due to an increase in aggregate size and/or flux. This negative adsorption is a physical rather than a chemical phenomenon, since it applies to both ^3H_2O and ^{36}Cl. For experiments carried out at a relatively small flux and in columns packed with small aggregates (column 1), both models yield similar estimates of the parameters P and R (Figures 1 and 2, Tables 2 and 3). For experiments 1, 2, and 3, the estimated ϕ is close to unity (Table 4). When ϕ is close to unity, models I and II are essentially the same. At a small flux the residence time (L/v_m) is apparently large enough for complete mixing to occur between mobile and immobile water regions in the medium, such that all water appears mobile if estimated from BTC.

Whereas model I failed to describe the BTC's of experiments 15–17, model II described the data well (Figures 5 and 6). For all displacements carried out through soil columns packed with aggregate fractions of either 1–2 mm or 2–4.7 mm (columns 2 and 3, respectively), model I fails to describe the data, especially the tailing of BTC's for both tracers (e.g., Figure 7 for ^{36}Cl). However, model II describes all BTC's (e.g., Figure 8). As far as model parameters are concerned, the Peclet numbers P and the retardation factors R of model I are smaller than those of model II for both tracers. This trend of data is emphasized in Figure 9 where P and R values from both models are compared. The optimization scheme used to estimate model parameters is such that it will force the model simulation to go through the data points as much as possible. Owing to the inadequacy of model I to describe solute transport through a porous medium with stagnant water, the model simulation will, as a matter of necessity, yield small P values and R values that show negative adsorption (Table 2) in order to shift the BTC's to the left. The apparent negative adsorption, as shown in Figures 2 and 7 and in Table 2, is due to a physical nonequilibrium situation that exists between the mobile and immobile water regions. R values of less than one are especially apparent for the larger aggregates (long diffusion path lengths) and the larger flux displacements (short residence times). A similar trend of parameters (P and R) was reported by *van Genuchten* [981] while using model I to describe ^{36}Cl transport through aggregated porous media. However, it is apparent that for small aggregates <2 mm and at small fluxes, model I describes symmetrical BTC's well. Similar observations were made by *van Genuchten and Wierenga* [1977], *Rao et al.* [1979, 1980*a*], and *DeSmedt* [1979]. Therefore the more complicated model II is not necessary when small particles are present or for displacements at small fluxes.

Since model I has proved unsuitable for describing solute transport through an aggregated porous medium, the dependence of model parameters on experimental conditions will be based on model II parameters. If a model parameter is

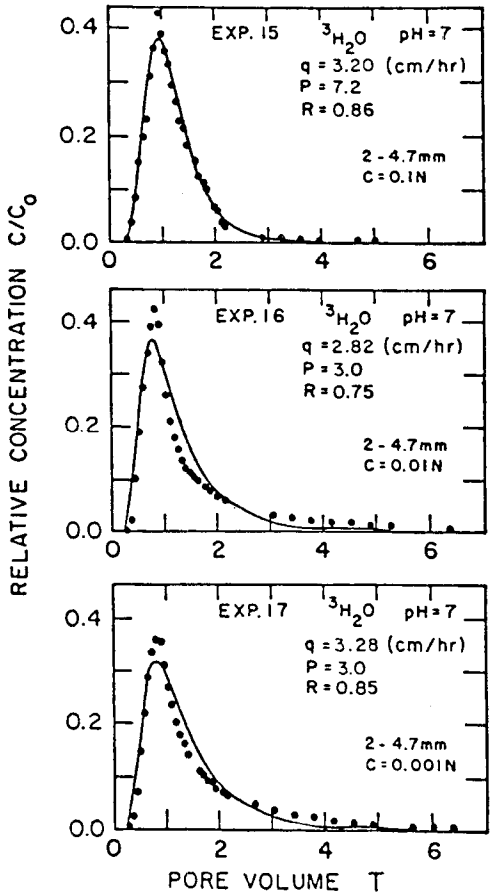

Fig. 3. Measured ^3H_2O breakthrough curves through column 3. The dots represent experimental data points, and the lines are calculated with model I.

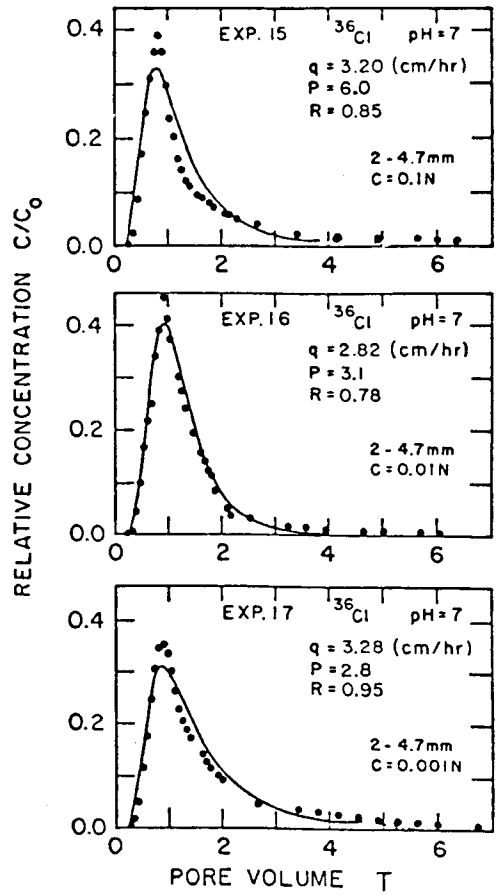

Fig. 4. Measured ^{36}Cl breakthrough curves through column 3. The dots represent experimental data points, and the lines are calculated with model I.

TABLE 4. Estimates of Original Variables From the Dimensionless Parameters of Model II

Experiment Number	ϕ		Average	D, cm^2 h^{-1}		K_D, ml g^{-1}		α, h^{-1}		Mobile Pore Water Velocity V_m, cm h^{-1}
	^{36}Cl	^3H_2O		^{36}Cl	^3H_2O	^{36}Cl	^3H_2O	^{36}Cl	^3H_2O	
1	0.90 ± 0.00	0.92 ± 0.01	0.91	0.67 ± 0.04	0.52 ± 0.03	0.034 ± 0.103	0.045 ± 0.006	0.06 ± 0.00	0.05 ± 0.01	0.48
2	0.91 ± 0.00	0.89 ± 0.06	0.90	0.65 ± 0.01	0.51 ± 0.03	0.059 ± 0.012	0.096 ± 0.007	0.05 ± 0.00	0.05 ± 0.03	0.49
3	0.67 ± 0.15	0.90 ± 0.00	0.79	0.56 ± 0.08	0.79 ± 0.05	−0.003 ± 0.011	0.058 ± 0.016	0.13 ± 0.03	0.04 ± 0.04	0.56
4	0.71 ± 0.23	0.84 ± 0.01	0.78	4.15 ± 0.95	3.98 ± 1.03	0.138 ± 0.011	0.127 ± 0.020	1.81 ± 1.69	1.22 ± 2.83	7.56
5	0.58 ± 0.02	0.65 ± 0.04	0.62	6.28 ± 0.09	8.49 ± 1.15	0.030 ± 0.019	0.036 ± 0.017	0.42 ± 0.66	0.31 ± 0.09	8.66
6	0.60 ± 0.02	0.61 ± 0.03	0.61	4.32 ± 0.33	5.38 ± 0.64	0.052 ± 0.013	0.088 ± 0.016	0.38 ± 0.05	0.38 ± 0.06	8.72
7	0.65 ± 0.03	0.75 ± 0.03	0.75	0.40 ± 0.05	0.43 ± 0.04	0.124 ± 0.022	0.086 ± 0.016	0.03 ± 0.01	0.02 ± 0.01	0.59
8	0.78 ± 0.00	0.96 ± 0.00	0.96	0.16 ± 0.02	0.17 ± 0.02	0.228 ± 0.019	0.147 ± 0.008	0.13 ± 0.02	0.05 ± 0.01	0.46
9	0.64 ± 0.06	0.71 ± 0.07	0.71	0.34 ± 0.05	0.41 ± 0.07	0.059 ± 0.059	0.066 ± 0.065	0.02 ± 0.01	0.01 ± 0.01	0.63
10	0.61 ± 0.03	0.69 ± 0.03	0.69	2.02 ± 0.34	2.28 ± 0.15	−0.025 ± 0.028	−0.041 ± 0.020	0.31 ± 0.06	0.21 ± 0.03	8.60
11	0.55 ± 0.04	0.72 ± 0.07	0.72	3.80 ± 0.23	4.02 ± 0.60	0.010 ± 0.039	0.086 ± 0.039	0.21 ± 0.00	0.14 ± 0.06	8.21
12	0.87 ± 0.14	0.72 ± 0.09	0.80	1.17 ± 0.17	0.70 ± 0.09	−0.056 ± 0.010	−0.039 ± 0.006	0.05 ± 0.06	0.09 ± 0.05	0.56
13	0.75 ± 0.07	0.87 ± 0.07	0.81	0.93 ± 0.06	0.87 ± 0.03	0.017 ± 0.030	−0.005 ± 0.028	0.02 ± 0.01	0.01 ± 0.01	0.54
14	0.64 ± 0.13	0.54 ± 0.05	0.59	0.42 ± 0.10	0.26 ± 0.04	0.093 ± 0.064	0.107 ± 0.025	0.03 ± 0.02	0.04 ± 0.01	0.75
15	0.81 ± 0.08	0.88 ± 0.07	0.85	4.03 ± 0.80	3.48 ± 0.80	−0.006 ± 0.027	−0.043 ± 0.020	0.14 ± 0.14	0.19 ± 0.33	6.54
16	0.44 ± 0.02	0.45 ± 0.01	0.45	3.78 ± 0.34	3.73 ± 0.33	0.149 ± 0.026	0.117 ± 0.019	0.41 ± 0.03	0.42 ± 0.02	10.88
17	0.47 ± 0.02	0.50 ± 0.03	0.49	4.12 ± 0.30	5.11 ± 4.80	0.177 ± 0.018	0.121 ± 0.022	0.62 ± 0.06	0.49 ± 0.03	11.03

sensitive to experimental conditions, that parameter is no longer a constant and cannot be used in model simulations for experimental conditions different than those from which it was obtained.

Model II contains four dimensionless parameters: P, R, β, and ω. Measured and fitted BTC's agreed well in all 17 experiments. The Peclet number P is the ratio of the characteristic times for hydrodynamic dispersion (L^2/D) and convection (L/v_m). The parameter P depends solely on the medium, provided the contribution to mixing by molecular diffusion is insignificant. For each column the apparent diffusion coefficient D increased with mobile pore water

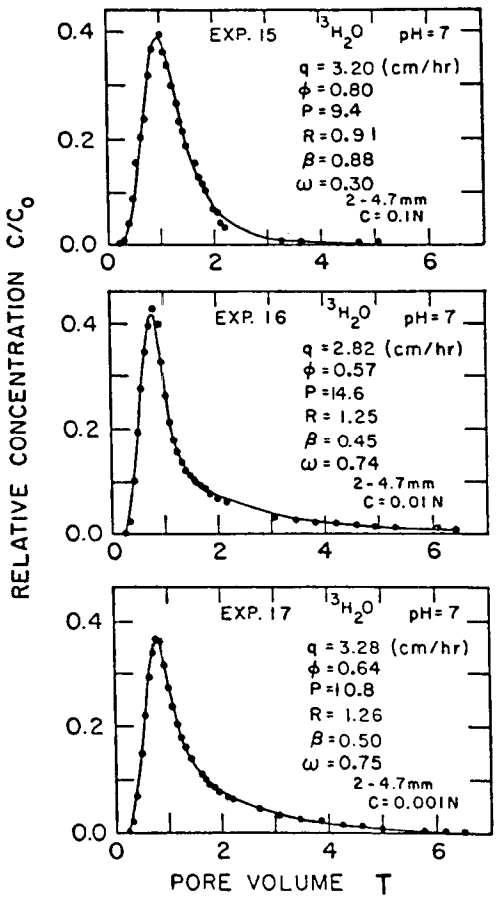

Fig. 5. Measured ^3H_2O breakthrough curves through column 3. The dots represent experimental data points, and the lines are calculated with model II.

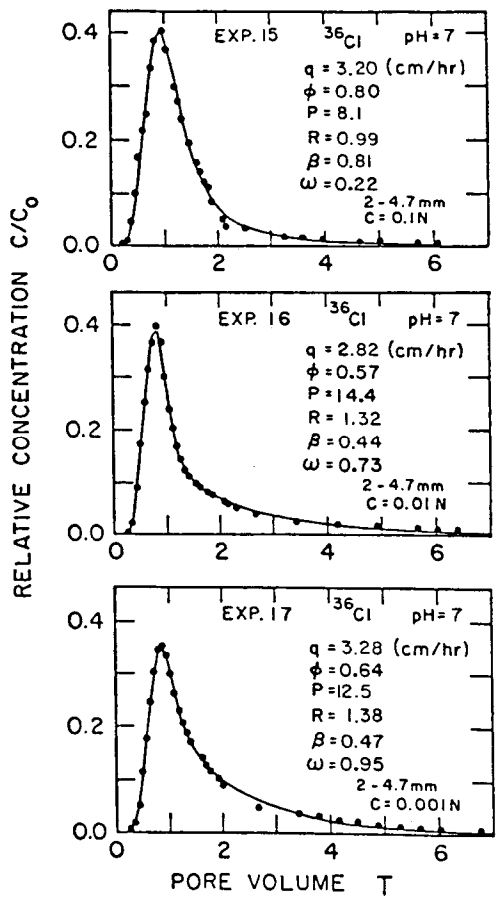

Fig. 6. Measured ^{36}Cl breakthrough curves through column 3. The dots represent experimental data points, and the lines are calculated with model II.

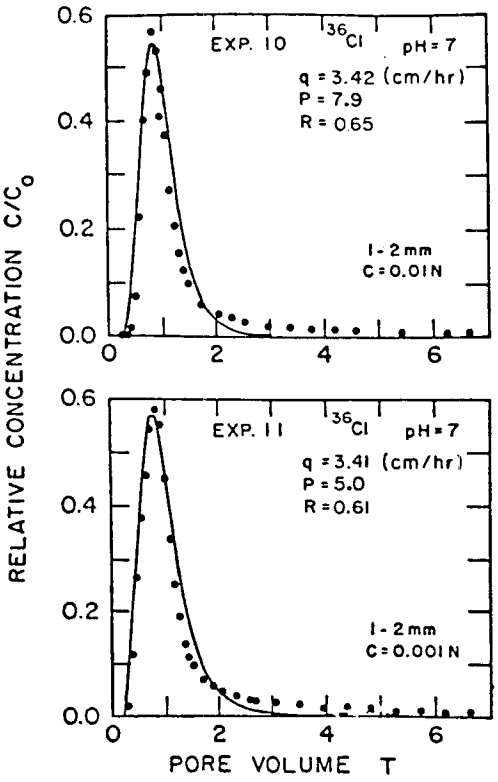

Fig. 7. Measured ^{36}Cl breakthrough curves through column 2. The dots represent experimental data points, and the lines are calculated with model I.

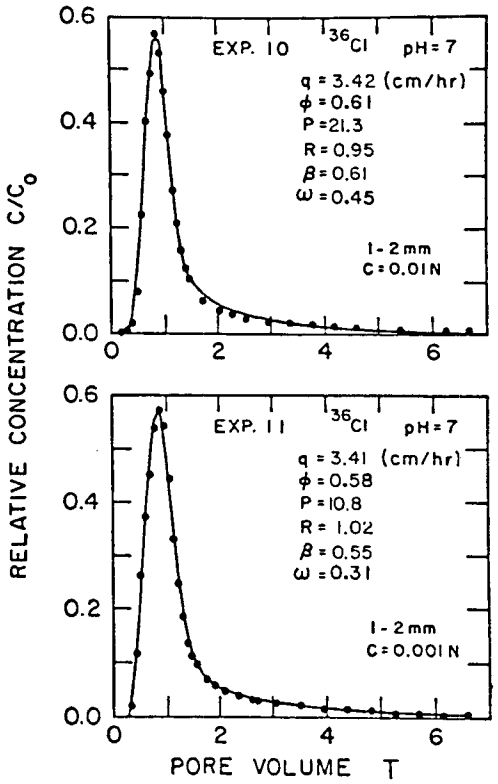

Fig. 8. Measured ^{36}Cl breakthrough curves through column 2. The dots represent experimental data points, and the lines are calculated with model II.

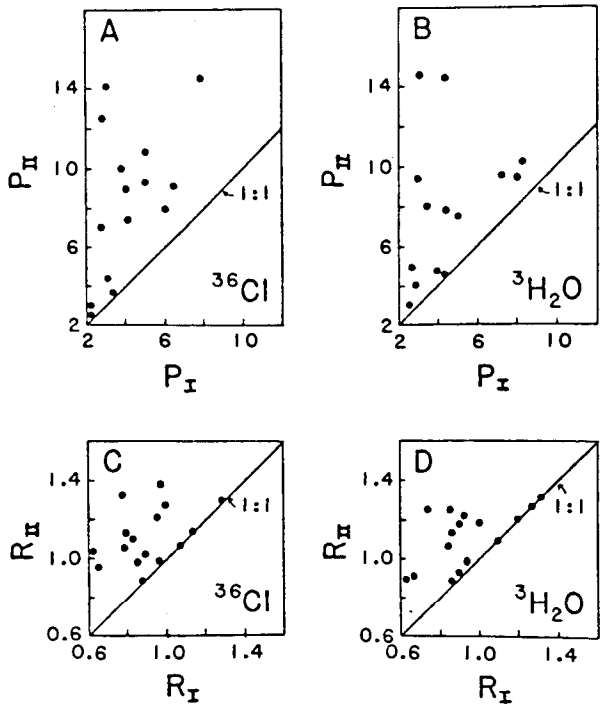

Fig. 9. A comparison of the Peclet number P and the retardation factor R estimated with model I and model II from ^3H_2O and ^{36}Cl breakthrough curves. (*a*) Peclet number with model I (P_I) and with model II (P_{II}) for ^{36}Cl. (*b*) Peclet number P for ^3H_2O. Retardation factors R for ^{36}Cl. (*d*) Retardation factors R for ^3H_2O.

velocity v_m for both tracers. The P values for both ^3H_2O and ^{36}Cl are similar (Table 3) even though both tracers have markedly different molecular diffusion coefficients. This suggests that convective transport in this study was more a function of physical characteristics of the porous medium and less of the diffusion properties of the tracer. In general, a single value of P could have been used for a given experiment for both ^3H_2O and ^{36}Cl. Furthermore, the correlation equations between D and v_m values from each column for all displacements are linear (Table 5). Thus for the range of flux used in this study, a single Peclet number could have been used for all displacements through the same column. The use of a constant P for all experiments run at different pore water velocities on the same column has been reported earlier [*van Genuchten and Wierenga*, 1977; *DeSmedt*, 1979; *Nkedi-Kizza et al.*, 1982]. A linear relationship between D and v_m has been reported earlier [*van Genuchten*, 1977; *DeSmedt*, 1979; *Coats and Smith*, 1964]. In this study, Peclet numbers estimated by curve fitting the data with model II were more

TABLE 5. Regression Equations Between D and v_m

Aggregate Size, mm	Tracer	Regression	R^2
0.5–1	^3H_2O	$D = 0.201 + 0.699\ v_m$	0.920*
0.5–1	^{36}Cl	$D = 0.343 + 0.552\ v_m$	0.963*
1–2	^3H_2O	$D = 0.153 + 0.354\ v_m$	0.913†
1–2	^{36}Cl	$D = 0.132 + 0.328\ v_m$	0.901†
2–4.7	^3H_2O	$D = 0.457 + 0.376\ v_m$	0.961*
2–4.7	^{36}Cl	$D = 0.811 + 0.316\ v_m$	0.931*

*Significant at the 1% level.
†Singificant at the 5% level.

or less insensitive to the various experimental conditions imposed on the same column.

The parameter R depends on the adsorption coefficient K_D, the bulk density ρ, and the moisture content θ. Therefore, R is determined by both the chemical under study and the characteristics of the porous medium. The R values for the different experiments are presented in Table 3 and K_D values are presented in Table 4 for both ^3H_2O and ^{36}Cl. Since for all experiments, ρ and θ values are almost constant (Table 1), R values should only be influenced by K_D. When examining Table 4, one finds that the average K_D value for both ^{36}Cl and ^3H_2O is 0.06 ± 0.07 ml g^{-1}, which is not significantly different from zero. Other researchers have reported tritium adsorption, especially in soils that contain large amounts of sesquioxides [*Biggar and Nielsen*, 1962; *Davidson et al.*, 1968; *van Genuchten and Wierenga*, 1977; *Nkedi-Kizza et al.*, 1982]. Since isotopic exchange is instantaneous, the differences in aggregate size and flux for the different experiments should not have affected the K_D values obtained. Since the K_D values are small, the variation in estimates of K_D from BTC's become more sensitive when the other parameters, especially β, have significant influences on the estimated BTC. For displacements through column 1 (experiments 1, 2, and 3) for which the parameter β is large and thus θ is close to unity, the K_D values are similar to what was obtained by *Nkedi-Kizza et al.* [1982], using batch studies, for the same soil.

The parameter β is dependent on the solute being transported and the physical and chemical characteristics of the porous medium. The mobile water fraction ϕ is related to β (equations (15) and (16)). In almost all cases the estimated ϕ value from the BTC's of ^3H_2O and ^{36}Cl are not significantly different (Table 4). The only exceptions are ϕ value for column 2. An average ϕ was therefore used in all calculations that involved ϕ. For column 2, displacement ϕ value for ^3H_2O were used instead of average ϕ in calculations that involved ϕ. The fraction of immobile water $(1 - \phi)$ surfaces (shown in Figure 10) illustrate the interaction between aggregate size, flux, and solution concentration on the estimated ϕ. The immobile water $(1 - \phi)$ seemed to increase with aggregate size and flux for displacements run with 0.001 N or 0.01 N $CaCl_2$ (Figures 10*a*, 10*b*). However, for displacements run with 0.1 N $CaCl_2$, the immobile water parameter is not sensitive to aggregate size and flux (Figure 10*c*). An independent measure of ϕ made by *Nkedi-Kizza et al.* [1982] from columns packed with Ione soil aggregates (2–4.7 mm) with soil solution of 0.01 N $CaCl_2$ was 0.60. The mobile water content ϕ for a given soil column and solution concentration estimated from BTC's is actually an 'apparent' ϕ, since it varies with flux (Figure 10). Increasing aggregate size at a given pore water velocity increases the diffusion path length, causing incomplete mixing between solutes in the mobile and immobile water regions. This, in turn, causes the solutes to appear early in the effluent. Similarly, a large pore water velocity provides a short residence time available for diffusive mass transfer of solutes into and out of the immobile water regions and yields an early breakthrough of the solute. Therefore, both large aggregates and high pore water velocities would result in large immobile water, if estimated from BTC's (Figure 10). The effect of solution concentration on ϕ could be attributed to changes that might occur in the proportion of macro- and micropores between aggregates as the solution concentration is varied from 0.1 N to 0.001 N $CaCl_2$. This decrease in concentration would increase the thickness of the electrical double layers such that some macropores in the system become micropores. This would result in an increase in $(1 - \phi)$. For displacements obtained with the greatest concentration of $CaCl_2$, the estimated ϕ appears to be independent of both particle size and flux (Table 4).

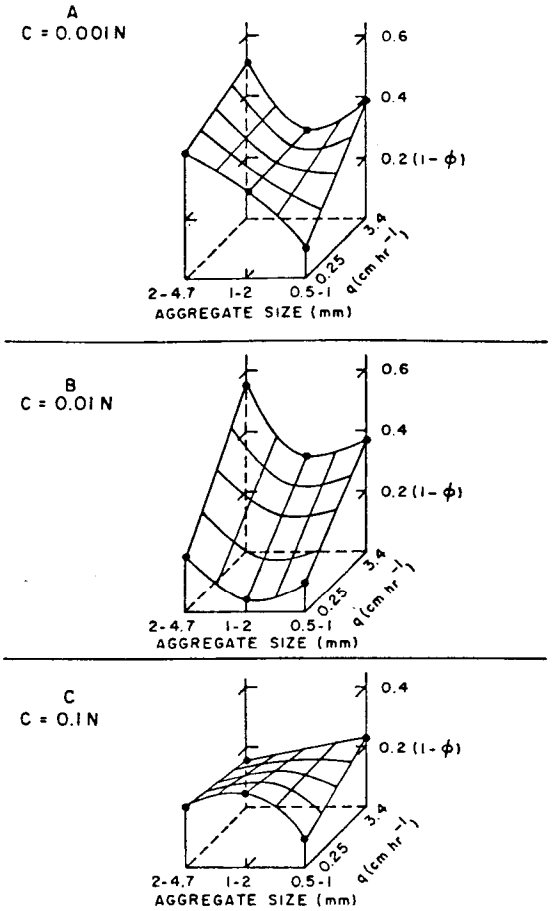

Fig. 10. Immobile water $(1 - \phi)$ as a function of aggregate size and flux. (*a*) Immobile water for displacements run with 0.001 N $CaCl_2$. (*b*) Immobile water for displacements run with 0.01 N $CaCl_2$. (*c*) Immobile water for displacements run with 0.1 N $CaCl_2$.

Figure 11 shows for both tracers that the mass transfer coefficient α increases with an increase in velocity. For α values estimated from BTC's obtained with 0.1 N $CaCl_2$, α decreases with an increase in aggregate size for both ^{36}Cl and ^3H_2O, respectively (Figures 11*c* and 11*f*). By using solution concentration of 0.1 N $CaCl_2$, *Rao et al.* [1980*a*, *b*] have theoretically and experimentally shown that α is not a constant but a function of the effective diffusion coefficient, aggregate size, mobile water content, and residence time. Similar results have been obtained in this study. The residence time is a measure of the length of time available for diffusion of solutes into and out of stagnant water regions during miscible displacement. The residence time is inversely related to pore water velocity; thus α should decrease with an increase in pore-water velocity, since α decreases with an increase in time over which it is calculated [*Rao et al.*, 1980*a*]. It is evident from Figure 11 that the mass transfer coefficient is sensitive to different values of the solution concentration. A clear understanding of the relation between

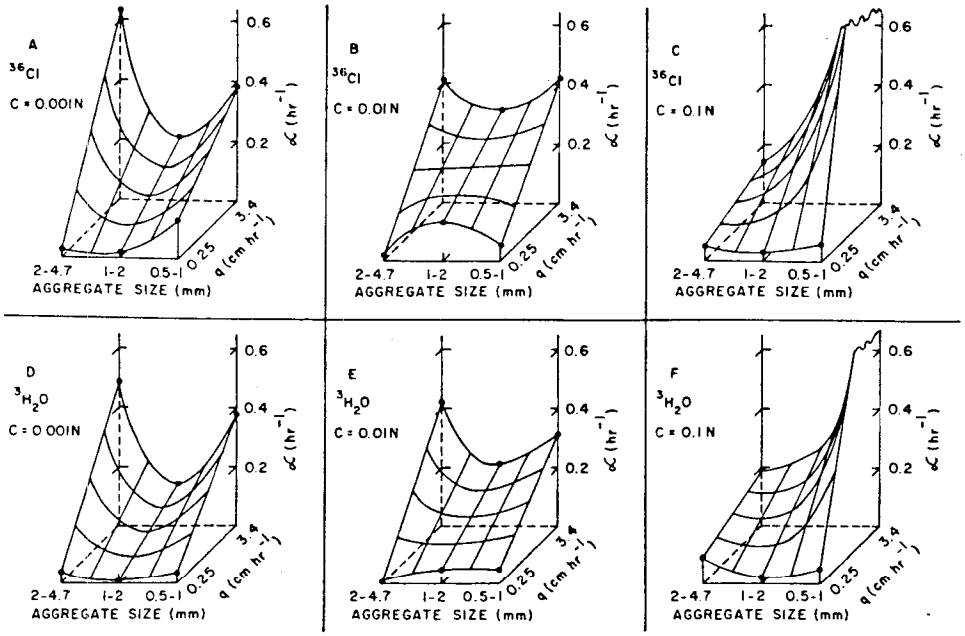

Fig. 11. The mass transfer coefficient α as a function of aggregate size and flux for ^{36}Cl and $^{3}H_2O$. (*a*) Value of α for ^{36}Cl for displacements run with 0.001 *N* $CaCl_2$. (*b*) Value of α for ^{36}Cl for displacements run with 0.01 *N* $CaCl_2$. (*c*) Value of α for ^{36}Cl for displacements run with 0.1 *N* $CaCl_2$. (*d*) Value of α for $^{3}H_2O$ for displacements run with 0.001 *N* $CaCl_2$. (*e*) Value of α for $^{3}H_2O$ for displacements run with 0.01 *N* $CaCl_2$. (*f*) Value of α for $^{3}H_2O$ for displacements run with 0.1 *N* $CaCl_2$.

α and the solution concentration will depend upon a more comprehensive study than the effort presented here.

Summary and Conclusions

Two conceptual models were evaluated for describing $^{3}H_2O$ and ^{36}Cl transport through a porous medium exhibiting physical nonequilibrium. In model I, all soil water was considered to be mobile. In model II, the soil-water phase was partitioned into mobile and immobile regions. Convective-diffusive solute transport was limited to the mobile water regions, and the diffusion controlled transfer of tracers into and out of the immobile water region was assumed to occur at a rate proportional to the concentration difference between the two water regions. Adsorption of $^{3}H_2O$ and ^{36}Cl in both models was assumed to be an instantaneous, linear, and reversible process.

Model I contains two independent parameters (P and R) and model II contains four parameters (P, R, β, and ω). They were all estimated by curve-fitting measured BTC data. For columns packed with small aggregates (0.5–1.0 mm), the BTC's obtained at a small flux (0.2 cm/h) were fairly symmetrical for both tracers and could be described equally well with both models. However, as the aggregate size and flux increased, model I failed to describe the experimental data, whereas the parameter R became less than one. This apparent negative adsorption was attributed to the inadequacy of model I to describe solute transport through porous media that exhibit physical nonequilibrium. To match the experimental BTC's with Model I simulations, both parameters P and R had to be small so as to shift the simulated BTC's to the left.

Model II describe all the experimental data well. This study revealed that the mobile water fraction ϕ estimated from BTC's is not a constant but a function of aggregate size, pore water velocity, and solution concentration. For small aggregates and for small pore water velocity experiments, ϕ estimated from BTC's was essentially equal to one. A decrease in concentration showed a decrease in ϕ. The mobile water generally decreased also with an increase in both aggregate size and flux. The mobile water calculated for both $^{3}H_2O$ and ^{36}Cl was similar. The diffusive mass transfer coefficient α in this study was a function of aggregate size, pore water velocity, and concentration. The variation of these two parameters ϕ and α with changes in experimental condition (e.g., flux and aggregate size) point out that although model II is the best available to describe solute transport through aggregated porous media, the model is and always will be an approximation of the physical system if parameters are estimated from BTC's.

A constant Peclet number P could have been used for both tracers for displacement experiments run through the same column since a linear relationship exist between D and v_m for both tracers. The retardation factor R can best be estimated from BTC's run at very slow fluxes, such R values can then be used to calculate BTC's run at larger fluxes. Similarly, the best estimate of ϕ can be obtained from BTC's run at very large fluxes for a given aggregate size. Thus, owing to the variation of model parameters with experimental conditions, the best estimate of these parameters will only be obtained from displacement experiments that are carefully designed to take into account the effect of the various factors addressed in this study.

Notation

C_0 input concentration, nCi/ml.

C_1 dimensionless solution concentration in the mobile region.

C_2 dimensionless solution concentration in the immobile region.

C_{im} average solution concentration in the immobile region, nCi/ml.
C_m average solution concentration in the mobile region, nCi/ml.
D apparent diffusion coefficient, cm^2/h.
D_0 molecular diffusion coefficient in bulk fluid, cm^2/h.
f fraction of adsorption sites in the mobile region.
K_D distribution coefficient for linear adsorption isotherm, ml/g.
L column length, cm.
P column peclet number.
q Darcy flow velocity, cm/h.
R retardation factor.
R_m retardation factor in the mobile region.
t time, h.
t_1 pulse time.
T pore volume equal to vt/L.
T_1 dimensionless pulse time, equal to vt_1/L.
v average pore water velocity, equal to q/θ; cm/h.
v_m average pore water velocity in mobile region, equal to q/θ_m; cm/h.
x dimensionless distance along the flow direction, equal to Z/L.
Z distance along the flow direction, cm.
α first order mass transfer coefficient, 1/h.
ω dimensionless mass transfer coefficient.
β dimensionless partition variable (equation (10)).
θ volumetric soil water content.
θ_{im} volumetric soil water content in the immobile region.
θ_m volumetric soil water content in the mobile region.
ρ bulk density, gm/cm^3.
ϕ fraction of soil water that is mobile.

REFERENCES

Biggar, J. W., and D. R. Nielsen, Miscible displacement, 2, Behavior of tracers, *Soil Sci. Soc. Am. Proc., 26,* 125–128, 1962.

Boyd, G. E., A. W. Adamson, and L. S. Myers, The exchange adsorption of ions from aqueous solutions by organic zeolites, 2, Kinetics, *J. Am. Chem. Soc., 69,* 2836–2848, 1947.

Coats, K. H., and B. D. Smith, Dead-end pore volume and dispersion in porous media, *Soc. Pet. Eng. J., 4,* 73–84, 1964.

Davidson, J. M., C. M. Reick, and P. W. Santelman, Influence of water flux and porous material on the movement of selected herbicides, *Soil Sci. Soc. Am. Proc., 32,* 629–633, 1968.

Davidson, J. M., P. S. C. Rao, R. E. Green, and H. M. Selim, Evaluation of conceptual models for solute behavior in soil-water systems, in *Agro-Chemicals in Soils,* edited by A. Banin and U. Kafkafi, Pergamon, New York, 1980.

DeSmedt, F., Theoretical and experimental study of solute movement through porous media with mobile and immobile water, Ph.D. dissertation. Vrije Universiteit, Fac. der Toegepaste Wetensch., Dienst Hydrol., Brussels, 1979.

DeSmedt, F., and P. J. Wierenga, Mass transfer in porous media with immobile water, *J. Hydrol., 41,* 59–67, 1979*a*.

DeSmedt, F., and P. J. Wierenga, A generalized solution for solute flow in soil with mobile and immobile water, *Water Resour. Res., 15,* 1137–1141, 1979*b*.

Gaudet, J. P., H. Jegat, C. Vachaud, and P. J. Wierenga, Solute transfer, with exchange between mobile and stagnant water, through unsaturated sand, *Soil Sci. Soc. Am. J., 41,* 665–671, 1977.

Gilliland, E. R., and R. F. Baddour, The rate of ion exchange, *Ind. Eng. Chem., 45,* 330–337, 1953.

Gottschlich, D. R., Axial dispersion in a packed bed, *Am. Inst. Chem. Eng. J., 9,* 88–92, 1963.

Hiester, N. K., and T. Vermeulen, Saturation performance of ion-exchange and adsorption columns, *Chem. Eng. Progr., 48,* 505–516, 1952.

Lapidus, L., and N. R. Amundson, The rate-determining steps in radial adsorption analysis, *J. Phys. Chem., 56,* 373–383, 1952.

Lindstrom, F. T., R. Haque, V. H. Fried, and L. Boersma, Theory on the movement of some herbicides in soils, *Environ. Sci. Tech., 1,* 561–565, 1967.

Nkedi-Kizza, P., Ion exchange in aggregated porous media during miscible emplacement, Ph.D. dissertation, Dep. of Land, Air, and Water Resour., Univ. of Calif., Davis, 1979.

Nkedi-Kizza, P., P. S. C. Rao, R. E. Jessup, and J. M. Davidson, Ion-exchange and diffusive mass transfer during miscible displacement through an aggregated Oxisol, *Soil Sci. Soc. Am. J., 46,* 471–476, 1982.

O'Connor, G. A., M. Th. van Genuchten and P. J. Wierenga, Predicting 2, 4, 5-T movement in soil columns, *J. Environ. Qual., 5,* 375–378, 1976.

Raats, P. A. C., Propagation of sinusoidal solute density oscillations in the mobile and stagnant phases of a soil, *Soil Sci. Soc. Am. Proc., 37,* 676–680, 1973.

Rao, P. S. C., J. M. Davidson, R. E. Jessup, and H. M. Selim, Evaluation of conceptual models for describing non-equilibrium adsorption-desorption of pesticides during steady-flow in soils, *Soil Sci. Soc. Am. J., 43,* 22–28, 1979.

Rao, P. S. C., D. E. Rolston, R. E. Jessup, and J. M. Davidson, Solute transport in aggregated porous media: Theoretical and experimental evaluation, *Soil Sci. Soc. Am. J., 44,* 1139–1146, 1980*a*.

Rao, P. S. C., R. E. Jessup, D. E. Rolston, J. M. Davidson, and D. P. Kilcrease, Experimental and mathematical description of non-adsorbed solute transfer by diffusion in spherical aggregates, *Soil Sci. Soc. Am. J., 44,* 684–688, 1980*b*.

Singer, M. J., and P. Nkedi-Kizza, Properties and history of an exhumed tertiary Oxisol in California, *Soil Sci. Soc. Am. J., 44,* 587–590, 1980.

Skopp, J., and A. W. Warrick, A two-phase model for the miscible displacement of reactive solutes through soils, *Soil Sci. Soc. Am. Proc., 38,* 544–550, 1974.

van Genuchten, M. Th., Non-equilibrium solute transport parameters from miscible displacement experiments, Res. Rep. 119, U.S. Salinity Lab. and Dep. of Soil and Environ. Sci., Univ. of Calif., Riverside, 1981.

van Genuchten, M. Th., and P. J. Wierenga, Mass transfer studies in sorbing porous media, 1, Analytical solutions, *Soil Sci. Soc. Am. J., 40,* 473–480, 1976.

van Genuchten, M. Th., and P. J. Wierenga, Mass transfer studies in sorbing porous media, 2, Experimental evaluation with tritium (^3H_2O), *Soil Sci. Soc. Am. J., 41,* 272–278, 1977.

van Genuchten, M. Th., P. J. Wierenga, and G. A. O'Connor, Mass transfer studies in sorbing porous media, 3, Experimental evaluation with 2, 4, 5-T, *Soil Sci. Soc. Am. J., 41,* 278–285, 1977.

(Received April 5, 1982;
revised February 7, 1983;
accepted February 25, 1983.)